

Higgs boson coupling measurements in ATLAS

Antonio Jesús Gómez Delegido^{a,1,*} on behalf of the ATLAS Collaboration

*^aInstitut de Física Corpuscular, CSIC-UV,
Carrer del Catedratic Jose Beltran Martinez, 2, Paterna, Spain*

E-mail: Antonio.J.Gomez@uv.es

The discovery of a Higgs boson with a mass around 125 GeV by the ATLAS and CMS experiments has opened a window into a fundamental sector of the Standard Model. Precise measurements of this new particle's properties provide essential tests of the Standard Model's consistency. This article presents a selection of measurements and searches performed by the ATLAS experiment, based on 140 fb^{-1} of $\sqrt{s} = 13 \text{ TeV}$ pp collision data collected during LHC Run 2. The latest determinations of Higgs boson couplings across various decay channels are reported, utilizing production mode cross-section measurements and the detailed kinematic description offered by the Simplified Template Cross Sections framework. Combinations of these results are also discussed.

*12th Large Hadron Collider Physics Conference (LHCP2024)
3-7 June 2024
Boston, USA*

¹The author acknowledges the support from the grant MCIN/AEI/PID2021-124912NB-I00 and the FPU 2019 grant funded by MCIN/AEI/10.13039/501100011033.

*Speaker

1. Introduction

In 2012, the ATLAS [1] and CMS [2] experiments at the LHC announced the discovery of a particle consistent with the Higgs boson as predicted by the Standard Model (SM) of particle physics [3, 4]. Since then, a central focus of particle physics has been to test the properties of this new particle, particularly its coupling strengths with other particles.

The Higgs boson interacts primarily through three types of couplings: gauge couplings with the W and Z bosons, which are essential for validating the mechanism of spontaneous symmetry breaking; Yukawa couplings with fermions, which are crucial for confirming the SM prediction that coupling strengths are proportional to the fermion mass; and the Higgs boson self-coupling, that constrains the Higgs potential.

During LHC Run 2, from 2015 to 2018, all major Higgs production and decay modes were successfully observed using a dataset of up to 140 fb^{-1} . Additionally, preliminary evidence for rare decays, such as $H \rightarrow \mu^+ \mu^-$ and $H \rightarrow Z\gamma$, began to emerge [5, 6]. Detailed measurements of Higgs couplings are critical for testing the SM's consistency. These proceedings present a series of ATLAS analyses that exploit the Run 2 dataset to further investigate the Higgs sector.

Recent measurements of the Higgs boson couplings to bosons are discussed in section 2. Measurements of inclusive and differential Higgs boson cross-sections in the $H \rightarrow b\bar{b}$ and $H \rightarrow \tau^+ \tau^-$ decay channels are presented in section 3. Searches for the rare Higgs boson decays into second-generation fermions are shown in section 4. Finally, the latest Higgs boson couplings measurements using a combination of ATLAS analyses targeting different signatures and decay modes are presented in section 5.

2. Couplings to bosons

The combination of measurements of many Higgs boson production and decay modes have determined the couplings of the Higgs boson with W (κ_W) and Z bosons (κ_Z) with an uncertainty below the 6% [7]. Furthermore, they have constrained the absolute value of the ratio of the coupling strengths $\lambda_{WZ} = |\kappa_W / \kappa_Z|$ to be consistent with 1, in agreement with the SM prediction. However, these measurements rely primarily on decays into WW^* or ZZ^* , vector-boson fusion (VBF) production, and associated production with a vector boson (WH and ZH , commonly referred as VH), all of which scale with the squares of κ_W and κ_Z . They can not determine the relative sign between them. Negative values of κ_W are excluded due to interference with the top quark in the loop-induced Higgs decay to $\gamma\gamma$. However, the combined measurements do not resolve the sign of κ_Z .

The ATLAS Collaboration has performed searches for VBF WH production [8], targeting two scenarios: a beyond Standard Model (BSM) scenario, where a negative λ_{WZ} results in constructive interference between diagrams, enhancing VBF WH production, and the SM scenario, where destructive interference is expected.

Both analyses target Higgs boson decays into pairs of bottom quarks and leptonically decaying W bosons. The event categorization defines not only signal-enriched regions but also control regions, where the normalization of the main backgrounds (such as $t\bar{t}$, single top production, and W +jets production) is extracted via a simultaneous fit to the data.

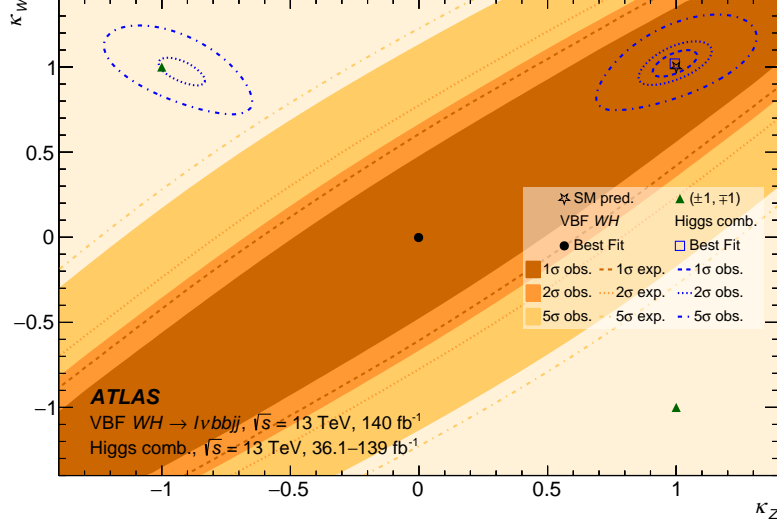


Figure 1: Fit results in the (κ_Z, κ_W) plane using the negative- λ_{WZ} analysis. The results are overlaid with confidence regions (shown in blue) from a separate fit that combines the Higgs boson measurements collected in Reference [7]. The SM value is marked with a star, while green triangles indicate the points with $\kappa_Z = \pm 1$ and $\kappa_W = \mp 1$ [8].

The non-SM hypothesis is excluded with a significance greater than 5σ , and the observed (expected) upper limits on the VBF WH cross-sections are 9.0 (8.7) times the SM prediction at 95% confidence level. The best-fit values for the λ_{WZ} , together with the confidence regions in the (κ_Z, κ_W) plane are shown in Figure 1.

3. Cross-sections measurements with Higgs boson decays into third-generation fermions

Experimentally well-understood Higgs decays, such as $H \rightarrow b\bar{b}$, with a branching ratio of 58%, can be useful for studying extreme corners of phase space. The analysis presented here performs the first measurement of boosted Higgs boson production associated with vector bosons, a measurement with high sensitivity to BSM effects [9]. The analysis targets the hadronic decays of vector bosons due to their larger branching fraction compared to semileptonic decays, probing higher values of Higgs boson transverse momentum.

The analysis selects events with a two large- R jet topology, where one of the large- R jets must satisfy $H \rightarrow b\bar{b}$ tagging requirements, while the other is required to pass W/Z tagging selections. The dominant multijet background is estimated using data-driven techniques. The other backgrounds are modeled through Monte Carlo (MC) simulations, with the normalization of Z +jets left as a free parameter in the fit. The VH production cross-section is measured inclusively and in different ranges of Higgs transverse momentum (p_T^H), yielding an observed significance of 1.7σ for the inclusive measurement under the null signal hypothesis. The distributions used to extract these cross-sections are shown in Figure 2.

The $H \rightarrow \tau^+\tau^-$ decay mode offers the best sensitivity to VBF Higgs boson production, due to the distinct VBF signature of two jets with a high invariant mass and the relatively large branching

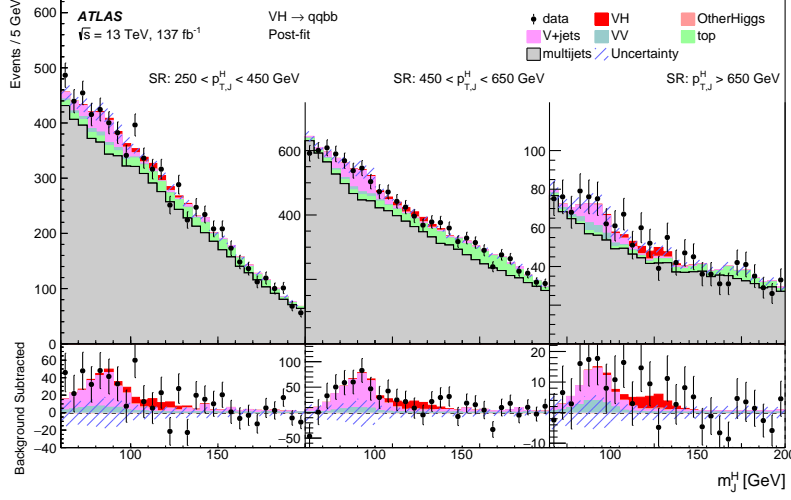


Figure 2: Distributions of the Higgs candidate jet mass (m_J^H) in the signal region are shown for three ranges of Higgs transverse momentum (p_T^H): $[250, 450)$ GeV (left), $[450, 650)$ GeV (middle), and $p_T^H \geq 650$ GeV (right). The variable m_J^H represents the invariant mass of the $b\bar{b}$ system, in which the Higgs boson candidate decays. A correction is applied to account for the energy carried by muons from semileptonic b -hadron decays, improving the mass resolution. The distributions are shown after performing an inclusive fit using a single Z +jets normalization factor and a single signal strength. The bottom panels present the distributions after subtracting the multijet and top-quark backgrounds. The hatched bands indicate the total uncertainty in the background estimate [9].

ratio of the $H \rightarrow \tau^+\tau^-$ decay. The results presented here are built on previous measurements [10], expanding the number of Simplified Template Cross Section (STXS) bins [11, 12] for VBF and $t\bar{t}H$ production while refining analysis techniques to enhance precision, particularly in those phase spaces [13]. The same strategy from Reference [10] is maintained for gluon-gluon fusion (ggF) and VH measurements.

The analysis categorizes events based on the τ decay modes into three channels: $\tau_{\text{had}}\tau_{\text{had}}$, $\tau_{\text{lep}}\tau_{\text{had}}$, and $\tau_{\text{lep}}\tau_{\text{lep}}$. The Higgs mass is reconstructed using the Missing Mass Calculator technique [14], which exploits information from the visible τ decay products and the missing transverse momentum to infer the neutrino momentum. Events are further split into different categories to provide sensitivity to the targeted STXS bins.

Eight kinematic bins are defined for VBF based on the invariant mass of the dijet system (m_{jj}) and the transverse momentum of the Higgs, while three signal regions are defined for $t\bar{t}H$, targeting different ranges of the Higgs p_T . A novel neural network trained with information from the di- τ system and missing transverse momentum, is used to reconstruct p_T^H for event categorization, leading to an approximate 50% improvement in p_T^H resolution. Further multivariate techniques are employed to enhance separation between signal and background events. For VBF, a boosted decision tree (BDT) is used to distinguish the VBF signal from ggF production and the leading $Z \rightarrow \tau\tau$ background. For $t\bar{t}H$, a multiclass BDT with three output nodes is applied to separate the $t\bar{t}H$ signal from $t\bar{t}$ and $Z \rightarrow \tau\tau$ backgrounds, defining signal and background-enriched regions.

The Higgs boson production cross-section is measured across 18 phase space regions within

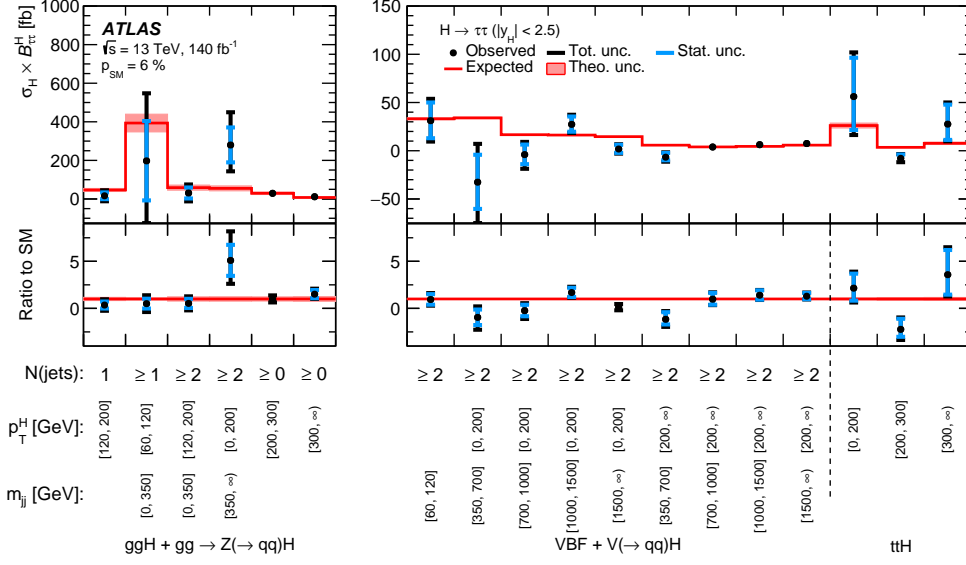


Figure 3: Measured values for cross-section times branching ratio in the $H \rightarrow \tau^+\tau^-$ STXS measurement. The total $\pm 1\sigma$ uncertainty in the measurement is shown with black error bars, while the blue bars indicate the individual contribution from statistical uncertainty [13].

the STXS framework, as shown in Figure 3. The measured values are in agreement with the SM expectations. The ratio of the measured cross-section to the SM prediction for $m_{jj} > 1500$ GeV and $p_T^H \geq 200$ GeV ($p_T^H < 200$ GeV) is $1.29^{+0.39}_{-0.34}$ ($0.12^{+0.34}_{-0.33}$), providing the first VBF measurement in the high- p_T^H phase space and the most precise in the case of the lower- p_T^H criteria.

4. Searches for rare Higgs boson decays

Searching for the $H \rightarrow \mu^+\mu^-$ and $H \rightarrow c\bar{c}$ decays mode allows exploring the coupling of the Higgs boson to second generation fermions.

The $H \rightarrow \mu^+\mu^-$ decay channel provides a direct probe of the Higgs boson coupling to second-generation leptons. Distinguishing the small SM-predicted $H \rightarrow \mu^+\mu^-$ signal from the large background from Drell-Yan production is an experimental challenge. In the analysis presented here [5], events are categorized to target different Higgs production modes, and the signal is extracted via a fit to the dimuon invariant mass ($m_{\mu\mu}$) spectrum. The dimuon invariant mass in all analysis categories is shown in Figure 4a. The observed (expected) significance over the background-only hypothesis is 2.0σ (1.7σ) for $m_H = 125.09$ GeV.

The search for $H \rightarrow c\bar{c}$ [15] is performed in a phase space that targets the VH production. This is a particularly challenging search due to the difficulty in distinguishing c -jets from other light-flavor jets. The c -tagging efficiency, which is approximately 27%, is crucial to the analysis. A simultaneous fit is performed on the $m_{c\bar{c}}$ spectrum in various event categories. The observed (expected) upper limit on the signal strength is 26 (31) times the SM prediction at 95% confidence level. These limits are shown in Figure 4b.

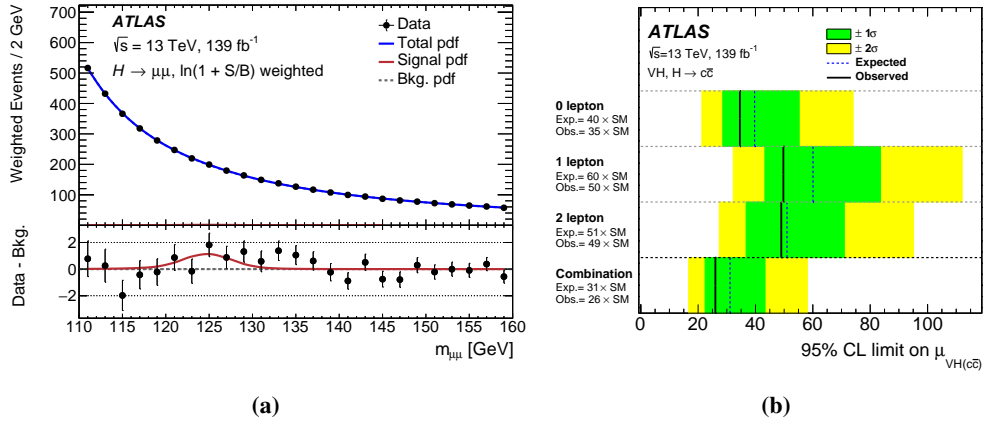


Figure 4: (a) Dimuon invariant mass spectrum in all analysis categories observed in data. Events are weighted by $\ln(1 + S/B)$, where S are the observed signal yields and B are the background yields derived from the fit to data in the $m_{\mu\mu} = 120\text{--}130$ GeV window. The background and signal probability density functions are derived from the fit to the data, with S normalized to its best-fit value. The error bars represent the data's statistical uncertainties [5]. (b) The observed and expected 95% confidence level upper limits on the cross-section times branching fraction normalized to the SM prediction in each analysis channel and for the combination of all the channels [15].

5. Cross-sections and couplings from combined fits

Measurements from different production and decay modes are often combined to improve the overall precision on Higgs boson properties.

The ATLAS collaboration has performed a detailed study of the Higgs boson cross-section for various production mechanisms, using approximately 140 fb^{-1} of data collected during Run 2 at a center-of-mass energy of $\sqrt{s} = 13 \text{ TeV}$ [7]. These total cross-section measurements access the Higgs boson primary production modes through six distinct decay channels: $b\bar{b}$, $\tau^+\tau^-$, $\mu^+\mu^-$, WW^* , ZZ^* , and $\gamma\gamma$. The measured cross-sections for the ggF and VBF processes achieve precisions of 7% and 12%, respectively. Additionally, the collaboration has detected the WH , ZH and $t\bar{t}H + tH$ process with observed signal significances above 5σ . The individual measurements of tH yield an upper limit on this production mode of 15 times the SM prediction at a 95% confidence level, compared to an expected limit of 7 times the SM prediction.

In this combination, measurements of Higgs boson cross-sections in specific phase space regions are performed using the STXS framework. The phase space is divided as a function of the jet multiplicity, p_T^H , and kinematic properties of the associated particles (such as vector bosons). This framework is designed to optimize the sensitivity to potential BSM effects by minimizing theory uncertainties and reducing model dependence in the measurements.

The STXS framework uses well-defined fiducial regions that can be compared across experiments and theoretical calculations, allowing for a more precise comparison between experimental data and SM predictions. This approach is particularly powerful for detecting small deviations from the SM or for probing extreme regions of phase space where new physics might manifest. Figure 5 provides a summary of the STXS measurements conducted by the ATLAS experiment combining different analyses, using the the Stage 1.2 STXS scheme.

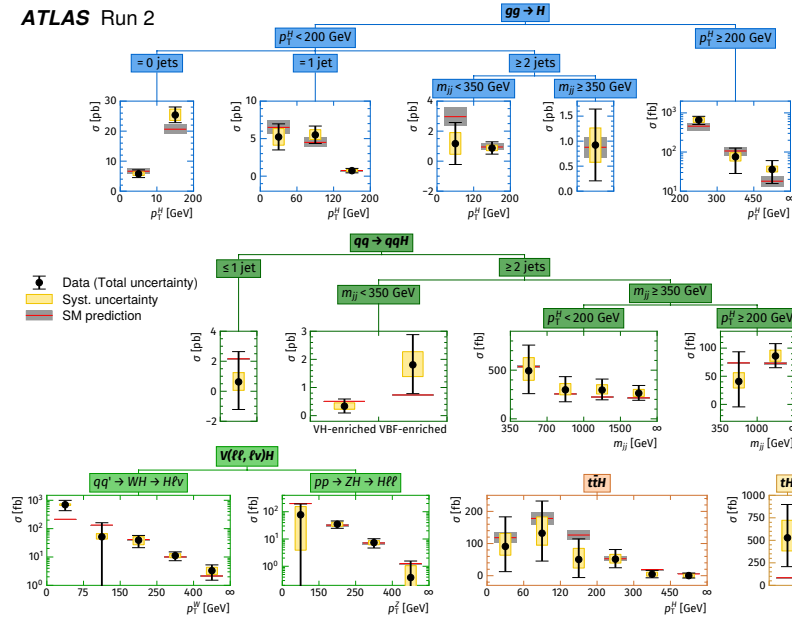


Figure 5: Observed and predicted Higgs boson production cross sections in different kinematic regions. The vertical bar on each point denotes the 68% confidence interval. The p -value for compatibility of the combined measurement and the SM prediction is 94%. Kinematic regions are defined separately for each production process, based on the jet multiplicity, the transverse momentum of the Higgs (p_T^H) and vector bosons (p_T^W and p_T^Z), and m_{jj} [7].

The combined analyses presented here demonstrate good agreement with the Standard Model, with no significant deviations observed. The measurements of cross-sections with the STXS framework are consistent with SM predictions, with p -values as high as 94%, indicating strong compatibility between the data and the SM expectations.

6. Conclusions

This document has presented recent ATLAS results, focusing on precision measurements of Higgs boson couplings and cross-sections. The measurements are in good agreement with the Standard Model predictions. Thanks to the larger Run 2 dataset and the advanced analysis techniques, uncertainties in coupling measurements have been reduced to below 10%. These improvements have enabled exploration of previously untested regions of phase space. Additionally, the ATLAS experiment is actively searching for rare decays of the Higgs boson, including those into second-generation fermions, further extending the understanding of the Higgs sector.

References

- [1] ATLAS Collaboration, *The ATLAS Experiment at the CERN Large Hadron Collider*, *JINST* **3** (2008) S08003.
- [2] CMS Collaboration, *The CMS Experiment at the CERN LHC*, *JINST* **3** (2008) S08004.
- [3] ATLAS Collaboration, *Observation of a new particle in the search for the Standard Model Higgs boson with the ATLAS detector at the LHC*, *Phys.Lett.B* **716** (2012) 1-29. [[hep-ex/1207.7214](#)].
- [4] CMS Collaboration, *Observation of a new boson at a mass of 125 GeV with the CMS Experiment at the LHC*, *Phys.Lett.B* **716** (2012) 30-61. [[hep-ex/1207.7235](#)].
- [5] ATLAS Collaboration, *A search for the dimuon decay of the Standard Model Higgs boson with the ATLAS detector*, *Phys.Lett.B* **812** (2021) 135980. [[hep-ex/2007.07830](#)].
- [6] ATLAS and CMS Collaborations, *Evidence for the Higgs Boson Decay to a Z Boson and a Photon at the LHC*, *Phys. Rev. Lett.* **132** (2024) 2, 021803. [[hep-ex/2309.03501](#)].
- [7] ATLAS Collaboration, *A detailed map of Higgs boson interactions by the ATLAS experiment ten years after the discovery*, *Nature* **607** (2022) 7917, 52–59. [[hep-ex/2207.00092](#)], Erratum: *Nature* **612** (2022) E24.
- [8] ATLAS Collaboration, *Determination of the Relative Sign of the Higgs boson couplings to W and Z Bosons Using WH Production via Vector-Boson Fusion with the ATLAS Detector*, *Phys. Rev. Lett.* **133** (2024) 14, 141801. [[hep-ex/2402.00426](#)].
- [9] ATLAS Collaboration, *Study of High-Transverse-Momentum Higgs Boson Production in Association with a Vector Boson in the qqbb Final State with the ATLAS Detector*, *Phys. Rev. Lett.* **132** (2024) 13, 131802. [[hep-ex/2312.07605](#)].
- [10] ATLAS Collaboration, *Measurements of Higgs boson production cross-sections in the $H \rightarrow \tau^+\tau^-$ decay channel in pp collisions at $\sqrt{s} = 13$ TeV with the ATLAS detector*, *JHEP* **08** (2022) 175. [[hep-ex/2201.08269](#)].
- [11] J. R. Andersen et al., *Les Houches 2015: Physics at TeV Colliders Standard Model Working Group Report*, *JHEP* **08** (2022) 175. [[hep-ph/1605.04692](#)].
- [12] N. Berger et al., *Simplified Template Cross Sections - Stage 1.1*, [[hep-ph/1906.02754](#)].
- [13] ATLAS Collaboration, *Differential cross-section measurements of Higgs boson production in the $H \rightarrow \tau^+\tau^-$ decay channel in pp collisions at $\sqrt{s} = 13$ TeV with the ATLAS detector*, [[hep-ex/2407.16320](#)].
- [14] A. Elagin, P. Murat, A. Pranko and A. Safonov, *A New Mass Reconstruction Technique for Resonances Decaying to di-tau*, *Nucl. Instrum. Meth. A* **654** (2011) 481–489. [[hep-ex/1012.4686](#)].

- [15] ATLAS Collaboration, *Direct constraint on the Higgs-charm coupling from a search for Higgs boson decays into charm quarks with the ATLAS detector*, *Eur. Phys. J. C* **82** (2022) 717. [[hep-ex/2201.11428](#)].